Published by
NIGERIAN SOCIETY OF PHYSICAL SCIENCES
Available online @ https://asr.nsps.org.ng/index.php/asr

African Scientific Reports 1 (2022) 103–114

African Scientific Reports

Extraction and Characterization of Pharmaceutical Grade Microcrystalline Cellulose From Bambara Nut (Voandzeia Subterranean (L) Thousars) Husk

E. Agboeze [a,*], N. P. Ani[a], E. O. Omeje[b]

[a]*Department of Industrial Chemistry, Enugu State University of Science and Technology, Enugu State, Nigeria*
[b]*Department of Pure and Industrial Chemistry, University of Nigeria Nsukka, Enugu State, Nigeria*

Abstract

Microcrystalline cellulose is a vital ingredient in the food, pharmaceutical, and cosmetics industries. In this study, Bambara nutshell microcrystalline cellulose (BNS-MCC) was prepared by acid hydrolysis modification of Bambara nutshell alpha-cellulose pulp. The sample was subjected to sodium hydroxide pulping (2.0% and 17.5% NaOH respectively) and a multistage pulping treatment using 3.5% nitric acid. The analysis results showed that the pulping method was effective for substantial removal of lignin with a 14. 416% yield of alpha-cellulose pulp. The organoleptic and physicochemical properties of BNS-MCC were examined. The prepared BNS-MCC powder was examined using a Scanning Electron Microscope (SEM), Fourier Transform Infrared spectroscopy (FTIR), and X-ray Diffractometer (XRD). The sample's powder flow properties (true density, Hausner index, Carr's index, angle of repose, powder porosity, loss on drying, and moisture sorption capacity) were (1.216g/mL, 1.34, 25.75%, 39.80^o, 64.7%, and 46.81%). The results of the analysis of the BNS-MCC compared well with commercial grades and conformed to US Pharmacopeia (USP) and British Pharmacopeia specifications. This result shows that Bambara nutshells have potential application for pharmaceutical grade cellulose production used in direct compression tableting.

DOI:10.46481/asr.2022.1.2.31

Keywords: Extraction, Characterization, Bambara nut husk, Microcrystalline cellulose

Article History :
Received: 03 May 2022
Received in revised form: 14 June 2022
Accepted for publication: 21 June 2022
Published: 29 August 2022

© 2022 The Author(s). Published by the Nigerian Society of Physical Sciences under the terms of the Creative Commons Attribution 4.0 International license. Further distribution of this work must maintain attribution to the author(s) and the published article's title, journal citation, and DOI.

Communicated by: Tolulope Latunde

*Corresponding author tel. no:

Email address: emmanuel.agboeze@gmail.com (E. Agboeze)

1. Introduction

Cellulose, a unique abundant renewable biopolymer on planet Earth, consists of linear homopolysaccharides and a structure of amorphous and crystalline region with β-(1→ 4) linked D-glucose repeating units. It is the main component of the cell wall of plants, which gives them structural support and acts as an element of reinforcement alongside hemicellulose and lignin. Cellulose in the last few decades has received tremendous research interest because of its availability and unique properties, which include mechanical and thermal stability, durability, biodegradability, non-toxicity, biocompatibility to the environment. Hence, its use in various applications, such as cosmetic, reinforcing polymer, pharmaceutical, and food industries [1, 2, 3]. Cellulose crystal structure, aspect ratio, and morphology have been reported to depend on the particle extraction process's source material and methodology of the particle extraction process [4, 5]. Crystalline cellulose is comparable to Kevlar, carbon fibers, and clay nanoparticles because of its high thermal and mechanical properties with 110-220 GPa elastic module in axial direction has also been reported [6, 7]. The development of cellulose modification by mineral acids to degrade the bulk of the amorphous region and reduce the cellulose fiber to microns yielded commercial forms of microcrystalline cellulose (MCC) [8]. MCC has been reported as purified, partly depolymerized cellulose prepared by treating α-cellulose pulp obtained from fibrous plant materials with excess mineral acid [9]. MCC is a fascinating cellulose derivative commercially produced for food pharmaceutical industries. MCC is considered a diluent with excellent binding properties, and this usage prompts its use mostly as a filler binder indirect tablet compression. At low concentrations, it is a great dry binder. MCC can efficiently bind other materials, especially poorly tabletable active pharmaceutical ingredients [10, 11].

Recently agricultural residuals have been employed in the preparation of commercial-grade MCC. However, these plant materials' chemical composition and structural organization may affect the composition of the α-cellulose extract and, subsequently, the crystallinity of the MCC produced [12]. Microcrystalline cellulose is considered the new environmentally friendly and sustainable option for a collection of materials like plastic and metals.

Due to the steady increase in demand for cellulose pulp and a subsequent decrease in wood availability, alternative sources for quality cellulose are being investigated. Agricultural wastes like Bambara Nutshell, cotton, elephant grass are excellent substitutes for wood. They are a potential low-cost supply of cellulose and other cellulose derivatives because of their availability, abundance, and renewability. Utilizing such agricultural waste residues will create a second income source for farmers. It will equally reduce and prevent pollution, especially air resulting from a residual agricultural burn. Based on this background, we study the use of Bambara nut shells as a source for the production of pharmaceutical-grade MCC.

Bambara nut (*Voandzeia subterranean (L) Thouars*) is a leguminous plant native to Africa, although it is occasionally grown in Asia. Bambara nut seed is processed mainly into flour prepared and consumed in the form of a pudding commonly known as 'Okpa.' Large inedible waste (Bambara offal and husk/shell) is gotten from Bambara nut processing. Bambara nutshells are by-products of milling the Bambara seeds into flour. In Nigeria, large amounts of shells/pods are discarded as wastes, large quantities of the husk are discarded as waste in Nigeria. This paper reports on the production and characterization of BNS-MCC (Bambara nutshell microcrystalline cellulose).

2. Materials and Methods

2.1. Materials

The Bambara nutshells used in this analysis were sourced from the Akwata market in Enugu North Local Government Area, Nigeria. The chemicals used include Sodium hydroxide, 3.5 % w/v, Nitric acid, sodium nitrite, hydrochloric acid, sodium hypochlorite as Jik (Reckitt and Colman LTD., Nigeria). All chemicals used were of analytical reagent grade.

2.2. Extraction of Cellulose

2.2.1. Sample pretreatment

The Bambara nutshell sample was manually sorted to remove foreign materials. The sample was sun-dried for two days and then oven-dried at 60^{o}C for 6 hours, followed by milling. The resultant sample powder was sieved and the portion passing through a 1.2 mm mesh sieve was extracted using toluene-ethanol (2:1v/v) until the extractive solvent was clear. The extractive-free powder was dried at room temperature in dust-free air.

2.2.2. Pulping /delignification

The method of Okhamafe and Azubuike with a little modification was used [13]. Pulping was done in batches of 100 g. About 100 g of extractive free sample powder was delignified using 1L 2 % w/v aqueous solution of sodium hydroxide at 80 ^{o}C in a stainless-steel container for 1 hour. Followed by thorough washing and filtration until neutral. The resultant sample residue from above was treated with IL of 3.5 % nitric acid containing 0.04 g of sodium nitrite for 2 hours in a stainless steel container placed in a water bath at 80 ^{0}C to remove lignin in the form of soluble nitrolignins and was followed by thorough washing and filtration [14, 15].

2.2.3. Bleaching

The resultant sample residue was bleached using 1:1 aqueous dilution of 3.5 % sodium hypochlorite at 90 ^{o}C for 10 mins. The resultant holocellulose was thoroughly washed and filtered. The resulting holocellulose was treated with 17.5 % w/v sodium hydroxide at 80^{o}C for 30 mins. The alpha-cellulose pulp obtained from above was washed thoroughly with water. The alpha-cellulose pulp was further whitened using 1:1 aqueous dilution of 3.5 % w/v sodium hypochlorite for 5 mins at 100 ^{0}C, followed by washing until the filtrate was clear. Excess water was manually squeezed out using a calico material, and the alpha-cellulose pulp was oven-dried at 50 ^{0}C [16].

2.3. Preparation of microcrystalline cellulose (BNS –MCC)

The method of Ohwoavworhua was used [17]. About 35 g of the resulting alpha Cellulose pulp was hydrolyzed in a pyrex beaker using 1.2 L 2.5 mol/dm^3 hydrochloric acid at 100 ^{o}C for 15 mins. The hot mixture was transferred into cold tap water and stirred vigorously using a spatula, and the mixture was left to stand overnight. The MCC obtained was washed thoroughly until neutral and dried at 50 ^{0}C for 60 mins followed by further milling, and the portion passing through a 0.8 mm sieve was stored in an airtight container [18].

2.4. Characterization of BNS-MCC powder

The physicochemical and powder properties analysis of MCC obtained from the Bambara nutshell sample was carried out using standard methods.

2.5. Physico-Chemical Properties Analysis

The organoleptic qualities (color, odor, and taste qualities), identification, solubility, pH, properties of MCC obtained from the Bambara nutshell sample were made according to British Pharmacopoeia 2004 specifications.

2.6. Identification

A standard test method for the determination of microcrystalline cellulose, according to [19], was used. 2 g of the BNS-MCC sample was subjected to iodinated zinc chloride solution. A violet-blue coloration indicates the powder as microcrystalline cellulose.

2.7. Solubility

The sample's solubility was tested in organic solvents (water, sodium hydroxide, ethanol, dilute HCl, and diethyl ether).

2.8. pH

The pH of the BNS-MCC was determined by shaking 1 g of the powder with 50 cm^3 distilled water for 5mins, and the pH of the supernatant was determined using a pH meter.

2.9. Fourier-transform Infrared Analysis

The functional groups present in the BNS-MCC were studied using Fourier transform infrared spectrophotometer [Buck 530IR] England. The transmittance method was used for this analysis. The Fourier-transform infrared spectrum of the BNS-MCC sample was recorded using a KBr disc. The sample was scanned between 4550 and 650 cm-^{1} at 8 cm-^{1} resolution.

2.10. X-ray Crystallinity

XRD patterns were obtained using a Bruker D8 (X-ray diffractometer) advanced equipment with Cu Kα radiation, variable divergence and anti-scatter slits (illuminated length = 10 mm), and a post-diffraction monochromator. Data were collected from 10 to either 75 or 90$^{?}$ 2θ, counting for 0.2 s at 25$^{?}$C intervals. The crystallinity index (CrI) based on the "Segal method" [20] was calculated from the height ratio between the intensity of the crystalline peak ($I_{200}-I_{am}$) and total intensity (I_{200}) after subtraction of the background signal. The data's nonlinear least-squares fitting was carried out using TOPAS (v4.2, Bruker AXS) with the crystalline component calculated from the cellulose I_β structure published by [21, 22]. Pseudo-Voigt line shapes were used for crystalline and amorphous cellulose peaks. A three-parameter 2^{nd} order polynomial function was used for the background and the degree of crystallinity calculated from calculated using the expression; [20, 23]

$$CrI = \frac{I_{200} - I_{am}}{I_{200}}, \tag{1}$$

where I_{200} is the intensity of the peak at about $2\theta = 22$

I_{am} is the intensity at $2\theta = 18$

2.11. Scanning electron microscopy (powder morphology)

The surface morphology determination of the BNS-MCC powder was carried out using Phenom Prox Scanning Electron Microscope by Phenom-World Eindhoven Netherland.

2.12. Powder properties characterization

2.12.1. True density

The true density, Dt, of BNS-MCC powder was determined using the liquid displacement method, xylene was used as the immersion fluid, and the true density of the sample was calculated using the equation:

$$\text{Dt} = \frac{w}{[(a+w)]} \text{ x SG}, \tag{2}$$

where:

SG is the specific gravity of xylene,

a is the weight of bottle + solvent,

b is the weight of bottle + solvent + powder.

2.12.2. Bulk density

About 15 g of BNS-MCC powder was placed in a 100 cm^3 measuring cylinder, the volume (V_o) occupied by the sample was noted. The bulk density of the sample was calculated using the equation:

$$\text{Density} = \frac{\text{Weight of cellulose}}{\text{Volume of cellulose}} \tag{3}$$

2.12.3. Tap density

The volume (V_{500}) occupied by 15 g of BNS-MCC after 500 taps on a laboratory bench was determined using;

$$\text{Density} = \frac{\text{Weight of cellulose}}{\text{Volume } (V_{500})\text{of cellulose}} \tag{4}$$

2.12.4. Particle size distribution

Test sieves within 780 μm to 154 μm were arranged in descending order. About 12.77 g of BNS-MCC powder was placed on the topmost sieve, and the sieve and its content were shaken for 5 minutes in a JINLING Shaker (China), and the weight of the powder was retained on each sieve was determined. The average diameter was calculated thus: [24]

$$\text{A.D} = \sum \frac{(\%X_r) \times (X_m)}{100}, \tag{5}$$

where A.D is Average Diameter, Xr is percentage retained, Xm is mean aperture.

2.12.5. Powder flow properties

Properties that determine the flowability of microcrystalline powder include the Hausner index, Carr's index, angle of repose, and powder porosity.

2.12.6. Hausner Ratio

Hausner index is a characteristic property that determines interparticle friction. The Hausner's index was obtained by finding the ratio of tap density to bulk density obtained above using the expression;

$$\text{Hausner's index} = \frac{\text{Tap density}}{\text{bulk density}} \tag{6}$$

2.12.7. Carr's index (degree of compressibility)

Carr's index shows the ability of a powder to diminish in volume. Carr's index of BNS_MCC powder was calculated using the values of bulk and tap densities obtained above.

% Compressibility was calculated thus;

$$\%\ \text{compressibility} = \frac{\text{Tap density} - - \text{bulk density}}{\text{Tap density}}\ \text{x}\ 100 \tag{7}$$

2.12.8. Angle of repose

The angle of repose, a, was tested using the fixed funnel and free-standing cone method [25, 26]. The funnel was clamped such that its tip was 2 cm above a graph paper placed on a flat surface. The BNS-MCC powder was poured carefully through the funnel till the peak of the cone formed got to the tip of the funnel. The mean diameter of the base of the cone's base was determined, and the angle of repose tangent was calculated using the expression:

$$\text{(Angle of repose) a}^{\circ} = \frac{\tan^{-1} 2h}{D}, \tag{8}$$

where h is the height of the heap of powder, D is the diameter of the base of the heap of powder.

2.12.9. Powder porosity

The powder porosity was obtained from the bulk and true density values when substituted into the equation: [19]

$$\text{e} = \frac{\text{B}_b}{\text{D}_t}\ \text{x}\ 100, \tag{9}$$

where B_b is the bulk density

I_t is the true density

e is the porosity

2.12.10. Loss on drying

About 5 g of BNS-MCC sample powder was deposited on a petri dish and dried in a laboratory oven at a temperature of 105 *o in a laboratory oven at* 105 *oesr was placed on a The Carr'* C until its weight was constant. The percentage moisture loss was obtained as the weight of moisture to the weight of sample ratio expressed as a percentage, mathematically; [18]

$$\text{Loss on drying} = \frac{\text{W}_2 - - \text{W}_3}{\text{W}_2 - - \text{W}_1}\ \text{x}\ 100, \tag{10}$$

where W_1 =Weight of petri dish

W_2 =Weight of sample + petri dish

W_3 =Weight of dry substance + petri dish

Table 1: Some physicochemical properties of BNS-MCC

Identification	Turns violet-blue with iodinated $ZnCl_2$
pH	6.2
Solubility test	
Distilled water	Insoluble
Dil NaOH (5%)	Slightly soluble
Dil HCL (5%)	Insoluble
Ethanol	Insoluble
Diethyl ether	Insoluble

2.12.11. Moisture sorption capacity

About 2 grams of BNS-MCC sample powder was weighed and spread evenly on a tarred petri dish. The petri dish and its content were placed in a desiccator containing distilled water in its reservoir (relative humidity RH = 100 %). The weight gained by the sample at the end of five days was recorded, and the amount of adsorbed water was calculated from the difference in weight [27].

2.12.12. Hydration Capacity

The Kornblum and Stoopak method was used. A 1 g quantity of BNS-MCC sample was placed in four 15 mL capacity centrifuge tubes, and each content was made up with 10 mL distilled water and then stoppered. The content was shaken using a JINLING Shaker (China) for two minutes, after which the contents were allowed to stand for 10 minutes. The mixture was centrifuged at 1000rpm for 10 minutes, the supernatant was decanted carefully, and the sediment was weighed. The hydration capacity was measured as a ratio of the sediment weight to the weight of the dry sample.

3. Results and Discussion

Multistage pulping was used to delignify the Bambara nutshell. This method resulted in a homogenous α-cellulose pulp from the sample, and this shows that the pulping method was effective for the substantial removal of lignin. 12.394 % yield of α-cellulose pulp was obtained per 100g sample. The BNS α-cellulose pulp was hydrolyzed further in an aqueous HCl solution to obtain BNS-MCC.

3.1. Physicochemical Properties of BNS-MCC Powder

The organoleptic properties of the BNS-MCC obtained were good as the material was granular, odorless, and white in color. The BNS –MCC sample turned violet-blue on reacting with iodinated zinc chloride; this identifies the powder as MCC. The pH of the BNS –MCC recorded 6.2, which is within the official range of 5 -7.5 (British Pharmacopeia 2004)**.** The results of the physicochemical properties of BNS-MCC are shown in Table 1.

3.2. Powder Properties Characterization

3.2.1. Scanning Electron Microscope (SEM)

The scanning electron microscopy (SEM) micrographs of Avicel PH 101 and BNS-MCC powder are shown in Figure 1(a) and (b). The SEM micrographs of BNS – MCC and Avicel PH101 consist of non-aggregated fibers. The shorter and rough fibers as seen in BNS–MCC may be attributed to the difference in the source of material and processing methods used. Figure 1a and Figure 1b compares the SEM micrographs of both BNS – MCC and Avicel pH 101 samples.

The fibers were collected with a 8,000 magnification, which means that the amplification of the BNS-MCC appearance was bigger by 8,000 as shown in Figure 1b. The accelerated voltage is 20.0KV which is pretty high. This is due to the sample's structural qualities and engineering. If the sample is a bit rigid to tolerate a higher voltage, the voltage of the sample will be greater to raise the resolution yield, and it won't influence the blurriness of the image. BNS-MCC particles were more regular and had a spherical shape with size, roughly 200μm. Differences in surface

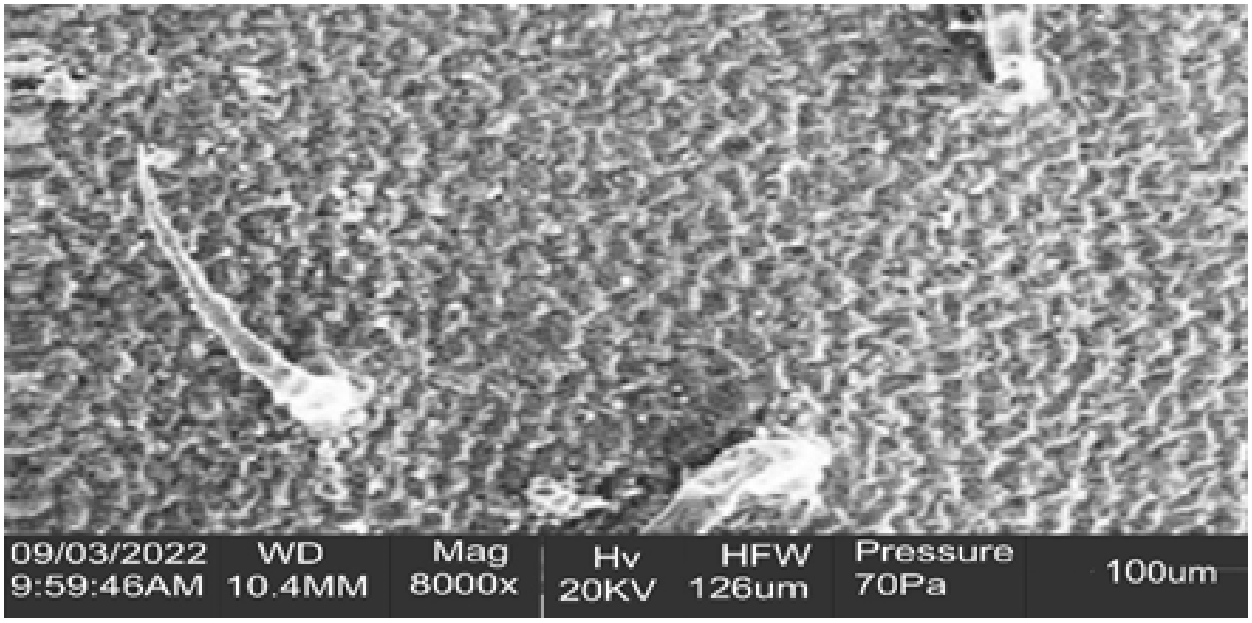
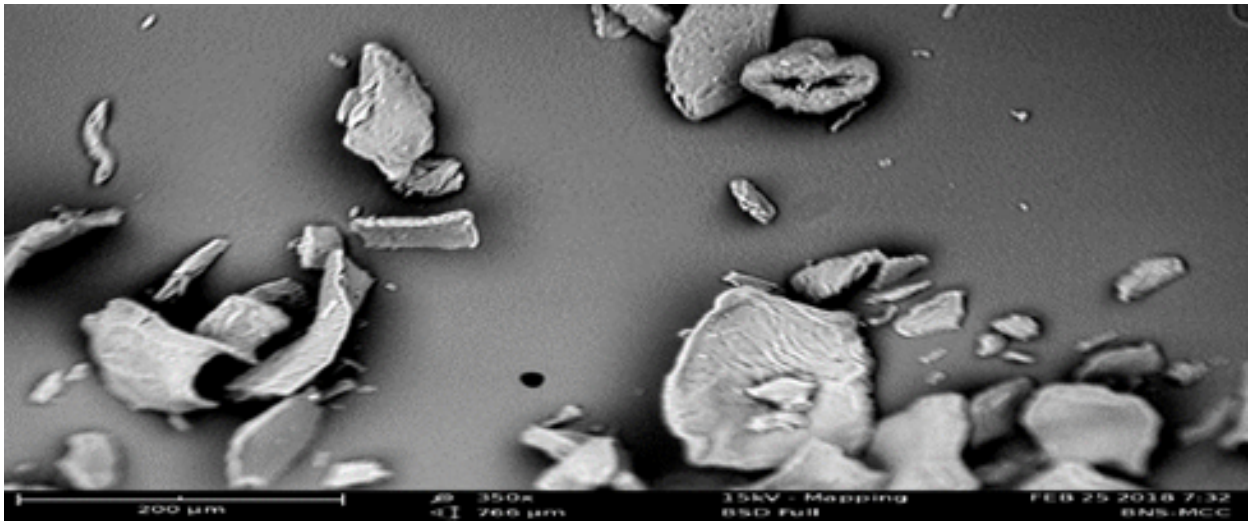


Figure 1: (a) SEM micrographs of Avicel pH 101



(b) SEM micrographs of BNS–MCC

morphologies were also evident. The higher magnifications revealed the surface structure of the BNS-MCC particles to be porous, formed by a web of fibrils. Such size and textural differences are apparent, expecting differences in particle rearrangement and, consequently, flow and compression behavior.

3.2.2. Energy dispersive X-ray spectroscopy (EDX)

Figure 2 shows the EDX images for BNS-MCC spectrum 1 in which the components and the concentrations are represented in weight percentages. The Figure shows the peaks of carbon, oxygen, Sulphur, and sodium corresponding to their binding energies. It consisted with mainly carbon with 64.5 wt% and Oxygen with 30% and low percentages of minor impurities of Sulphur 3.8 wt% and 1.7 wt% of Na. These impurities are the result of the bleaching and acid hydrolysis processes, in which Na is present in the NaClO acid used in the bleaching process and Sulphur is present

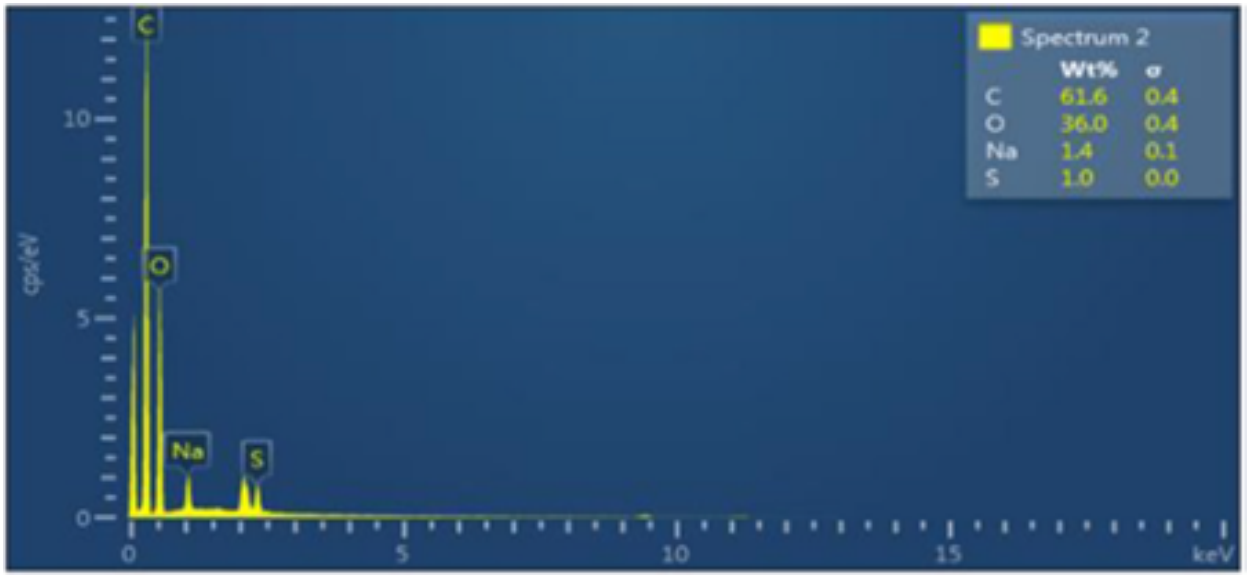


Figure 2: Analysis of BNS-MCC spectrum in EDX

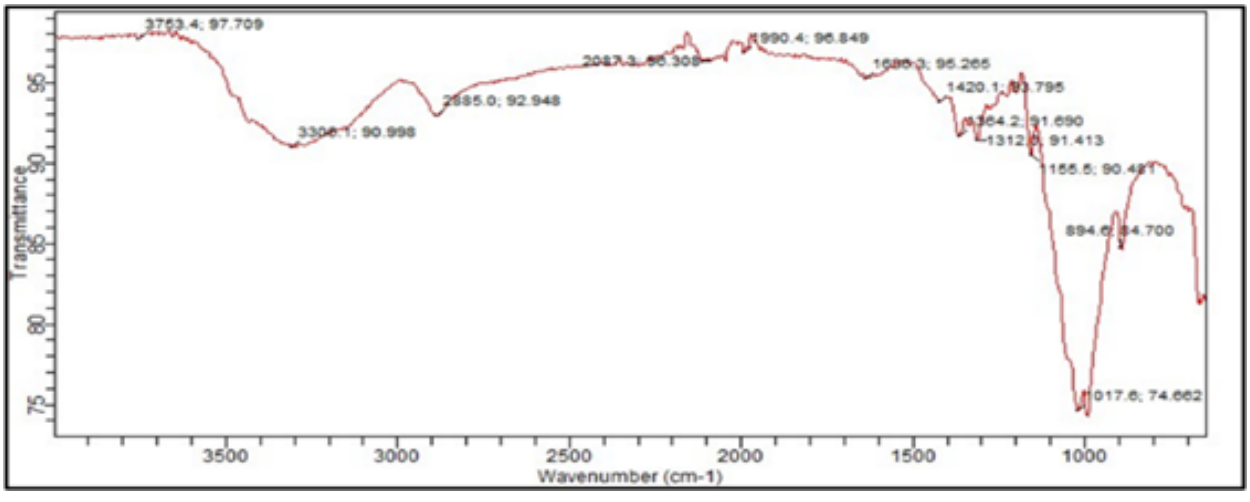


Figure 3: FT-IR spectrum of BNS-MCC

in the H_2SO_4 acid used in the acid hydrolysis process. Despite the fact that dialysis was carried out for several days, it appears that Sulphur and sodium were present to some amount.

3.2.3. Fourier Transform Infrared spectroscopy (FTIR)

The FT-IR spectrum of BNS-MCC in Figure 3 below show the characteristic spectrum of cellulose. Broad absorption at 3300.1cm^{-1} is assigned to different intermolecular and intramolecular O-H stretching vibrations. A peak at 1420.1, 1312.0cm^{-1} is assigned to intermolecular C-H symmetric bending vibrations. The peak at 894.7cm^{-1} is due to the stretching vibration of the C-H and C-O-C groups. According to Kassing, an increase in the intensity of this peak means

a decrease in the crystallinity of the cellulose material. The most complex region of FTIR spectra is the fingerprint region from 1430 cm^{-1} to approximately 850 cm^{-1}, which contains signals from the numerous sp^3 single bond vibrational modes. However, between 850 and 400 cm^{-1} is the region containing multiple bands corresponding to

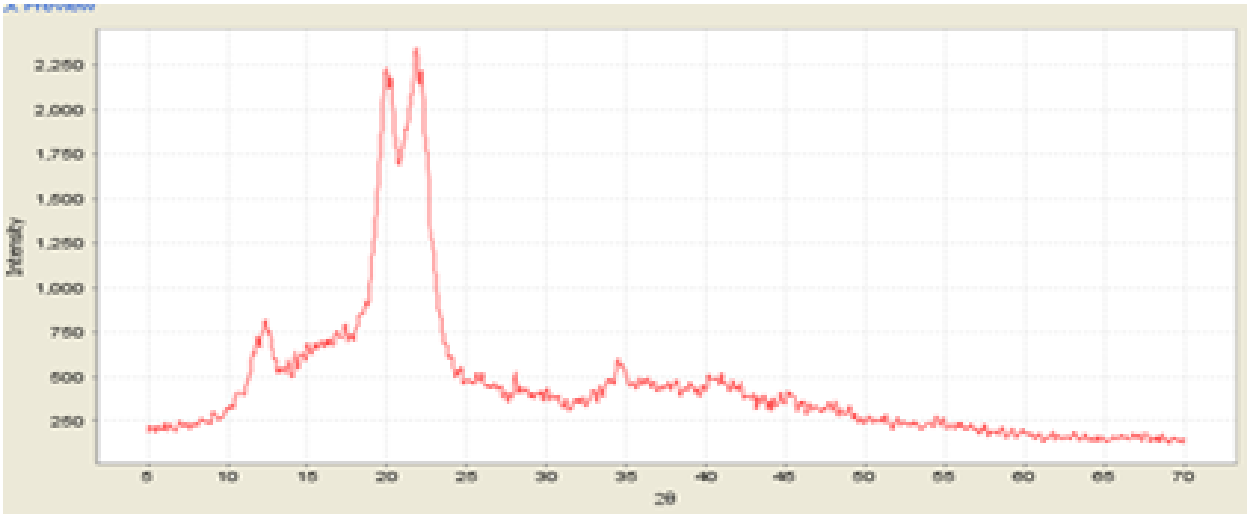


Figure 4: X-ray diffractogram BNS-MCC

heavy-atom bending and rotation.

Finally, an increase in the intensity from 80.916 obtained in BNS alpha-cellulose to 84.7 obtained in BNS-MCC indicates a change in crystal lattice from cellulose I to cellulose II [28, 29].

3.2.4. XRD

The x-ray diffractogram of the sample, as shown in Figure 4 below, is characteristic of cellulose II with peaks appearing at about 12.5^0, $20.0^{0,}$ and 22.0^0 at 2θ (as a result of 101 and 002 reflections) [9]. The calculated crystallinity index is 0.66, within the range of 0.58-0.69 reported by [9] for 11 brand-names MCCs.

3.2.5. Particle Size distribution

The particle size of BNS-MCC ranges from about 100-500 microns, with about 97% of the particle population less than 154 μm. Particle size depends upon the extent of degradation of cellulose molecule [30]. Finer particle size BNS-MCC promotes tablet (compact) strength as confirmed by the researchers. Variability in excipient particle size and content uniformity impacts on tablet hardness, friability and disintegration [31]. The particle size distribution of BNS-MCC is shown in [Figure 5].

It represents a unimodal frequency distribution that is negatively skewed

3.3. Powder flow properties

Bulk density depends on the particles packing behavior which changes as the powder consolidates [32]. Higher bulk density implies the need for larger amount for compressing tablet which is favourable in tableting due to reduction in the fill volume or so-called lower loading volume. The bulk density recorded 0.429, slightly above the USP specification of 0.32 (USP 32 – NF27), and the tapped density recorded 0.577. The flowability of MCC powder determines its suitability as a direct compression binder. Powder flowability is measured by the Hausner index, Carr's index, and angle of repose [29]. The higher the values of these parameters, the lower (poorer) the flow properties of the powder [33]. Table 2 shows the flow properties of the BNS – MCC powder.

Value in bracket represent standard deviation with n=3

Hausner's index shows interparticle friction; a value greater than 1.25 shows poor flow [34]. Hausner's index for the BNS-MCC recorded 1.34.

Carr's index (compressibility index) shows the ability of a material to reduce in volume, and any value less than 16% indicates good flow while values above 35 % show cohesion. BNS –MCC recorded a compressibility index of 25.75 % while the angle of repose recorded 39.80^o. The values of both Hausner's and Carr's indices and angle of repose shows that BNS – MCC flowed poorly according to the flowability scale in Table 3, but had better flow

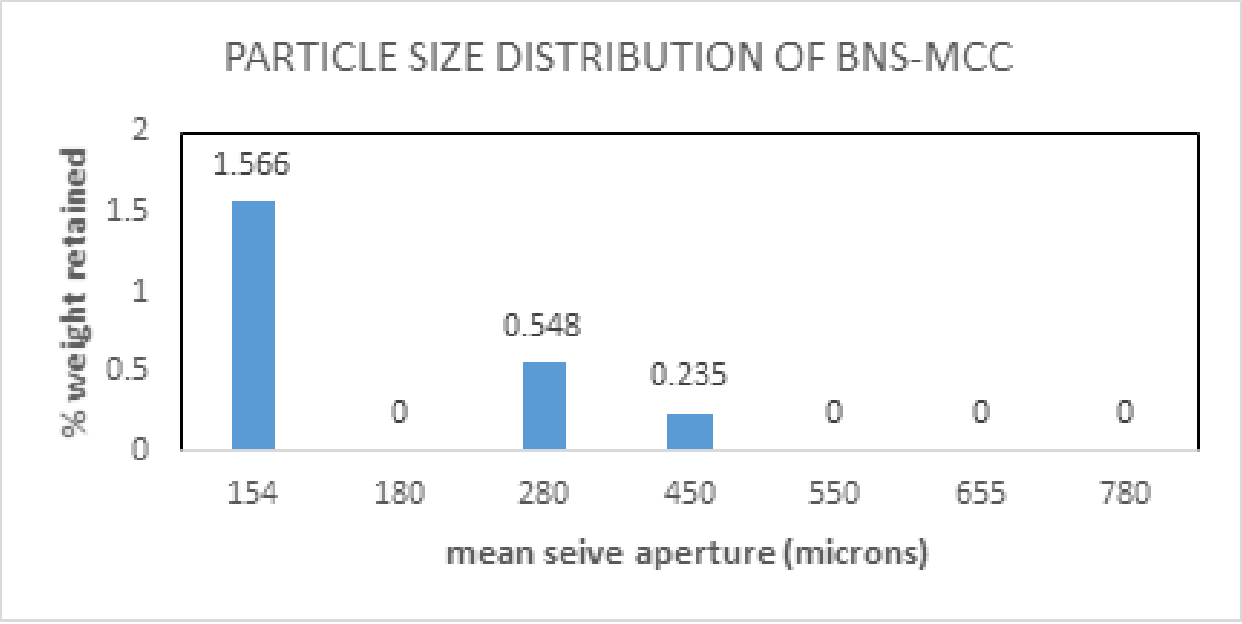


Figure 5: Particle size distribution of BNS-MCC

Table 2: Powder flow properties

Parameter	Results
True density g/mL	1.216
Bulk density g/mL	0.429
Tap density g/mL	0.577
Hausner's index	1.34
Carr's index %	25.75
Angle of repose	39.80°
Powder porosity %	64.7
Loss on drying %	5.89
Moisture sorption capacity %	46.81
Hydration capacity	2.80 (0.29)

Table 3: The scale of flowability

Carr's index	Hausner index	Angle of repose	Flow character
10	1.00-1.11	25-30	Excellent
11-15	1.12-1.18	31-35	Good
16-20	1.19-1.25	36-40	Fair
21-25	1.26-1.34	41-45	Passable
26-31	1.35-1.45	46-55	Poor
32-37	1.46-1.59	56-65	Very poor
>38	>1.60	>66	Very very poor

properties when compared with three MCCs obtained in literature examples GH – MCC (1.47, 31.72), [16] MCC – PP (1.379, 27.33) [35], CP – MCC (1.65, 39.5) [19] respectively. However, a glidant will be required to improve the flowability when using BNS–MCC in solid dosage forms formulations.

The loss on drying of BNS-MCC was 5.89% which is below the official limit of 6% (BP, 2004); this low value

indicates the suitability of BNS-MCC as a diluent in the formulation of hydrolyzable drugs.

Moisture sorption capacity measures a material's sensitivity to moisture, and this measurement is important because it shows the physical stability of tablets made with cellulose when stored under humid conditions. However, the moisture sorption capacity value for BNS-MCC was 36.8% which is too high and is indicative that BNS-MCC has a high proportion of amorphous cellulose as the amount of water adsorbed by cellulose is proportional to the amount of amorphous cellulose present. This shows that tablets made from BNS-MCC will be less stable. As a result, cellulose powders should be stored in airtight containers because of their sensitivity to atmospheric moisture. The hydration capacity value of BNS-MCC is indicative that its capable of absorbing more than two times its weight of water.

4. Conclusion

This work shows that the production of pharmaceutical-grade MCC from Bambara nut Shell is technically possible. The BNS-alpha cellulose pulp and BNS-MCC powder results were compared well with commercial-grade microcrystalline cellulose. They conformed well with USP specifications and British Pharmacopeial. Such an agricultural waste like Bambara nut Shell is a potential low-cost source of microcrystalline and cellulose derivatives, which can be employed in direct compression tableting and other pharmaceutical uses.

Acknowledgments

We thank the referees for the positive enlightening comments and suggestions, which have greatly helped us in making improvements to this paper.

References

[1] X. Shao, J. Wang, Z. Liu, N. Hu, M. Liu & Y. Xu, "Preparation and Characterization of Porous Microcrystalline Cellulose from Corncob", Industrial Crops and Products **112457** (2020).
[2] B. Sun, M. Zhang & Y. Ni, "Use of sulfated cellulose nanocrystals towards stability enhancement of gelatin-encapsulated tea polyphenols", Cellulose **25** (2018). 1.
[3] N. Y. Abu-Thabit, A. A. Judeh, A. S. Hakeem, A. Ul-Hamid, Y. Umar & A. Ahmad, "Isolation and characterization of microcrystalline cellulose from date seeds (Phoenix dactylifera L.)", International Journal of Biological Macromolecules **155** (2020) 1.
[4] B. Deepa, E. Abraham, N. Cordeiro, M. Mozetic, A. P. Mathew, K. Oksman & L. A. Pothan, "Utilization of various lignocellulosic biomass for the production of nanocellulose: a comparative study", Cellulose **2** (2015) 1.
[5] D. Haldar & M. K. Purkait, "Micro and nanocrystalline cellulose derivatives of lignocellulosic biomass: A review on synthesis, applications and advancements", Carbohydrate Polymers **116937** (2020) 1.
[6] B. Ates, S. Koytepe, A. Ulu, C. Gurses & V. K. Thakur, "Chemistry, structures, and advanced applications of nanocomposites from biorenewable resources", Chemical Reviews (2020) 1.
[7] R. J. Moon, A. Martini, J. Nairn, J. Simonsen & J. Youngblood, "Cellulose nanomaterials review: structure, properties and nanocomposite", Chemical Society Reviews (2011) 3941.
[8] J. N. BeMiller, "One hundred years of commercial food carbohydrates in the United States", Journal of Agricultural and Food Chemistry **18** (2009) 8125.
[9] R. Rowe, P. Sheskey & M. Quinn, *Handbook of Pharmaceutical Excipients*, London: Pharmaceutical Press (2009).
[10] A. Y. Chaerunisaa, S. Sriwidodo & M. Abdassah, "Microcrystalline Cellulose as Pharmaceutical Excipient. In Pharmaceutical Formulation Design-Recent Practices", IntechOpen (2019) 1.
[11] G. Thoorens, F. Krier, B. Leclercq, B. Carlin & B. Evrard, " Microcrystalline cellulose, a direct compression binder in a quality by design environment—A review", International journal of pharmaceutics **473** (2014) 64.
[12] G. Thoorens, F. Krier, E. Rozet, B. Carlin & B. & Evrard, " Understanding the impact of microcrystalline cellulose physicochemical properties on tabletability", International journal of pharmaceutics **490** (2015) 47.
[13] C. P. Azubuike & A. O. Okhamafe, "Physicochemical, spectroscopic and thermal properties of microcrystalline cellulose derived from corn cobs", International Journal of Recycling of Organic Waste in Agriculture (2012) 1.
[14] A. O. &. A. C. P. Okhamafe, "Direct compression studies on low-cost cellulose derived from maize cob", J. Pharm. Sci. Pharm. Pract. **2** (1994) 26.
[15] K. C. Ugoeze, N. Nwachukwu & P. C. Anyino, "The Effect of Modification Methods on the Properties of Lentinus Tuber Regium Powders", Journal of Pharmaceutical Technology, Research and Management **7** (2019) 27.
[16] F. O. Ohwoavworhua, T. A. Adelakun & A. O. Okhamafe, "Processing pharmaceutical grade microcrystalline cellulose from groundnut husk: Extraction methods and characterization.", International Journal of Green Pharmacy (IJGP) **3** (2009) 1.
[17] F. O. Ohwoavworhua, O. O. Kunle & S. I. Ofoefule, "Extraction and characterization of microcrystalline cellulose derived from Luffa cylindrica plant", African Journal of Pharmaceutical Research and Development **1** (2004) 1.
[18] F. O. Ohwoavworhua & T. A. Adelakun, "Some physical characteristics of microcrystalline cellulose obtained from raw cotton of Cochlospermum planchonii", Tropical Journal of Pharmaceutical Research **4** (2005) 501.

[19] D. K. Sidiras, D. P. Koullas, A. G. Vgenopoulos & E. G. Koukios, "Cellulose crystallinity as affected by various technical processes", Materials Science Paper & Wood (1990).
[20] A. D. French, "Idealized powder diffraction patterns for cellulose polymorphs.", Cellulose **21** (2014) 885.
[21] W. Schutyser, A. T. Renders, S. Van den Bosch, S. F. Koelewijn, G. T. Beckham & B. F. Sels, "Chemicals from lignin: an interplay of lignocellulose fractionation, depolymerisation, and upgrading", Chemical Society Reviews **47** (2018) 852.
[22] S. M. Fadel, W. S. Abou-Elseoud, E. A. Hassan, S. Ibrahim & M. L. Hassan, "Use of sugar beet cellulose nanofibers for paper coating", Industrial Crops and Products **180** (2022) 114787.
[23] L. Allen & H. C. Ansel, *Ansel's pharmaceutical dosage forms and drug delivery systems*, New York: Lippincott Williams & Wilkins (2013).
[24] D. Train, "Some aspects of the property of angle of repose of powders", Journal of Pharmacy and Pharmacology **10** (1958) 127T.
[25] A. F. Tarchoun, D. Trache & T. M. Klapotke, "Microcystalline cellulose from Posidonia oceanica brown algae: Extraction and characterization", International Journal of Biological Macromolecule **138** (2019) 837.
[26] M. Rouabah, S. Bourgeois, S. Briançon & C. Cogné, "A numerical tool to predict powder behaviour for pharmaceutical handling and processing", Journal of Drug Delivery Science and Technology **70** (2022) 103258.
[27] J. D. Audu-Peter, J. E. Ojile & P. G. Bhatia, "Physicochemical and powder properties of alpha-and microcrystalline-cellulose derived from maize cobs.", Journal of Pharmacy & Bioresources **1** (2004) 41.
[28] L. H. Zaini, M. Jonoobi, P. M. Tahir & S. Karimi, "Isolation and characterization of cellulose whiskers from kenaf (Hibiscus cannabinus L.) bast fibers", (2013) 1.
[29] H. A. Krassig, *Cellulose: Structure, Accessibility, and Reactivity, Yverdon*: Gordon and Breach Science (1993).
[30] M. H. Sainorudin, N. A. Abdullah, M. S. A. Rani, M. Mohammad, M, Mahizan, N. Shadan, N. H. A. Kadir, Z. Yaakob, A. El-Denglawey & M. Alam, "Structural characterization of microcrystalline and nanocrystalline cellulose from Ananas comosus L. leaves: Cytocompatibility and molecular docking studies", Nanotechnology Reviews **10** (2021) 793.
[31] X. Yue, J. He, T. Li & Y. Xu, "Preparing lignin-rich microcrystalline cellulose from spruce chemithermomechanical pulp fiber by Fe3+ enhanced high temperature liquid water treatment", Cellulose **28** (2021) 1405.
[32] J. Nsor-Atindana, M. Chen, H. D. Goff, F. Zhong, H. R. Sharif & Y. Li, "Functionality and nutritional aspects of microcrystalline cellulose in food", Carbohydrate Polymers **172** (2017) 159.
[33] R. C. Rowe, P. Sheskey & M. Quinn, *Handbook of pharmaceutical excipients*, Libros Digitales-Pharmaceutical Press, (2009).
[34] M. M. Haafiz, S. J. Eichhorn, A. Hassan & M. Jawaid, "Isolation and characterization of microcrystalline cellulose from oil palm biomass residue", Carbohydrate Polymers (2013) 628.
[35] C. C. Nwajiobi, J. O. E. Otaigbe & O. Oriji, "Physicochemical, spectroscopic and tableting properties of microcrystalline cellulose obtained from the African breadfruit seed hulls", African Journal of Biotechnology **18** (2019) 371.